Journal of Photochemistry, 13 (1980) 269 - 294

SINGLET AND TRIPLET STATES IN THE *cis–trans* PHOTOISOMERIZATION OF 4-CYANOSTILBENES IN SOLUTION

HELMUT GÖRNER

Institut für Strahlenchemie im Max-Planck-Institut für Kohlenforschung, D-4330 Mülheim a. d. Ruhr (F.R.G.)

(Received January 3, 1980)

Summary

The quantum yields of fluorescence ϕ_f, *cis*→*trans* photoisomerization $\phi_{c\rightarrow t}$ and *trans*→*cis* photoisomerization $\phi_{t\rightarrow c}$, and photostationary *trans/cis* ratios of 4-cyanostilbene, 4,4′-dicyanostilbene, 4-cyano-4′-methoxystilbene and 4-cyano-4′-dimethylaminostilbene were measured in several solvents as functions of quencher (ferrocene, azulene and oxygen) concentration, temperature and viscosity. The results suggest a singlet pathway for the direct *trans*→*cis* photoisomerization of the cyanostilbenes.

Photosensitized *cis–trans* isomerization and triplet energy transfer measurements were performed at room temperature for 4-cyano-4′-methoxystilbene. A transient was observed by laser flash photolysis for *trans* isomers of 4-cyanostilbene, 4,4′-dicyanostilbene and 4-cyano-4′-methoxystilbene at high viscosities. On decreasing the temperature and thus increasing the viscosity the yield ϕ_T and lifetime τ_T of the transient increase, reaching constant values in rigid media where $\phi_{t\rightarrow c}$ is almost zero. The viscosity independence of the transient spectrum and the temperature dependences of ϕ_T and τ_T lead to the identification of the transient as the planar *trans* configuration of the lowest triplet state. Contribution of this triplet state and possibly of a higher excited triplet state to the *trans*→*cis* photoisomerization is suggested to be very small even at low temperatures.

1. Introduction

In previous work differing pathways have been suggested for the *trans*→*cis* photoisomerization of 4-cyano-4′-methoxystilbene (CMS) and 4-nitro-4′-methoxystilbene (NMS) [1 - 10]. It has been shown that for NMS the direct *trans*→*cis* photoisomerization at room temperature occurs by a triplet mechanism, *i.e.* intersystem crossing to a planar *trans* triplet state, establishment of an equilibrium between the lowest planar and twisted triplet configurations and intersystem crossing to the twisted ground state followed by further twisting about the central double bond into the *cis* ground state [6, 9]. A

2.5. Materials

Trans isomers of CS, DCS, CMS and CDMAS were prepared and purified using methods described in the literature [20, 21]. For CS, DCS and CMS the *cis* isomers were produced by irradiation of the *trans* isomers until the photostationary state was established and by subsequent separation using high pressure liquid chromatography (Perkin Elmer, series 3, detector LC 55).

The purity of the cyanostilbenes was found by gas chromatography to be better than 99%. The sensitizers used were the same as those employed previously [7] with the addition of xanthone (Fluka, 99%), thioxanthone (Fluka, zone refined 99.5%), 2-acetonaphthone (Eastman, 99%) and acridine (Fluka, 98%); ferrocene (Merck, 99.8%) was recrystallized, and azulene (Aldrich, 99.3%) and 9,10-diphenylanthracene (EGA-Chemie, 99%) were used without further purification. The solvents (Merck) were purified by distillation where necessary. The preparation of the *trans*-cyanostilbenes in polymethyl methacrylate (PMMA) has been described elsewhere [22].

3. Results

3.1. Direct cis–trans *photoisomerization*

It has been shown in previous work that the effect of solvent polarity on the position of the photostationary state is significant for NMS but is small for CMS [3]. The *trans/cis* ratio in the photostationary state was measured for the four cyanostilbenes in several solvents at room temperature. A comparison of these values with those for the corresponding nitrostilbenes [23 - 25] is given in Table 1. The photostationary *trans/cis* ratios show only a slight solvent dependence for CS, DCS, NS and DNS. However, substitution of a methoxy or a dimethylamino group in the 4′ position leads to different results. On increasing solvent polarity the position of the photostationary state is slightly shifted to the *trans* form for the 4-cyanostilbenes but is strongly shifted to the *trans* form for NMS and 4-nitro-4′-dimethylaminostilbene (NDMAS).

The photostationary *trans/cis* ratio depends on the molar extinction coefficients ϵ_t and ϵ_c at the wavelength λ_{irr} of irradiation and on the quantum yields of direct photoisomerization (eqn. (1)):

$$\left(\frac{[t]}{[c]}\right)_s = \frac{\epsilon_c}{\epsilon_t} \frac{\phi_{c \to t}}{\phi_{t \to c}} \tag{1}$$

Values for $\phi_{t \to c}$ and $\phi_{c \to t}$ are listed in Table 2. Formation of 4*a*,4*b*-dihydrophenanthrene (DHP) from *cis*-cyanostilbenes may reduce $\phi_{c \to t}$. For CS in cyclohexane a quantum yield ϕ_{DHP} of 0.003 has been reported [20]. Comparably small yields for cyclization were found under prolonged irradiation conditions for CS, CMS and CDMAS in benzene and methanol by UV and gas chromatographic analyses. Only for DCS was a larger yield of DHP (in the absence of oxygen) and phenanthrene (in the presence of oxygen) found.

TABLE 1

Comparison of photostationary *trans/cis* ratios for cyanostilbenes and nitrostilbenes in solution at room temperature[a]

Compound	*Solvent*[b]	$([t]/[c])_s$		*Reference*[c]
		$R \equiv CN$	$R \equiv NO_2$	
4-R-stilbene	Cyclohexane	0.18	0.18	11
	Benzene	0.25	0.14	11
	Chloroform	0.25(0.3)[d]		
	Methanol	0.18	0.19	11
	Glycerol triacetate	0.22	0.22	8
4,4'-Di-R-stilbene	Cyclohexane	0.21		
	Benzene	0.22	0.12	11,23
	Chloroform	0.22(0.2)[d]	0.20	23
	Methanol	0.19	0.14	11,23
	Glycerol triacetate	0.21	0.18	8
4-R-4'-methoxystilbene	Cyclohexane	0.18[0.25][e]	0.17	6
	Benzene	0.14[0.28][e]	0.25	11,23
	Chloroform	0.20(0.2)[d]	0.79	23,24
	Methanol	0.16[0.30][e]	0.75	9,23
	Dimethylformamide	0.17	3.3	9,11
	Glycerol triacetate	0.19	0.59	8
4-R-4'-dimethylaminostilbene	Cyclohexane	0.22	0.90	23
	Benzene	0.28	14	23
	Methanol	0.22	>100	11,23
	Dimethylformamide	0.4	>100	23
	Glycerol triacetate	0.25	>100	8

[a]For CS and DCS λ_{irr} = 313 nm; for the other stilbenes λ_{irr} = 366 nm.
[b]Deoxygenated solutions.
[c]References refer to nitrostilbenes.
[d]Values in parentheses refer to oxygen at a pressure of 50 bar.
[e]Values in square brackets taken from ref. 3.

TABLE 2

Quantum yields of direct *trans→cis* and *cis→trans* photoisomerization for cyanostilbenes in solution at room temperature[a]

Compound	*Solvent*[b]	$\phi_{t\to c}$	$\phi_{c\to t}$	$(\%\ cis)_s$
CS	Cyclohexane	0.55 (0.46)[c]	0.45 (0.41)[c]	85 (81)[c]
	Benzene	0.42	0.45	80
	Ethanol	0.55	0.45	85
DCS	Cyclohexane	0.45	0.35[d]	83
	Ethanol	0.45	0.35[d]	84
CMS	Cyclohexane	0.45	0.40	85
	Benzene	0.40	0.40	88
	Ethanol	0.42	0.40	86
CDMAS	Cyclohexane	0.50	0.3[d]	82
	Benzene	0.50	0.3[d]	78
	Ethanol	0.55	0.3[d]	82

[a]For CS and DCS λ_{irr} = 313 nm; for the other stilbenes λ_{irr} = 366 nm.
[b]Deoxygenated solutions.
[c]Taken from ref. 25.
[d]Obtained from values for $\phi_{t\to c}$ and $([t]/[c])_s$ using eqn. (1).

3.1.1. Effects of quenchers on the photostationary state

Ferrocene, azulene and oxygen were used as quenchers of the *cis*⇄*trans* photoisomerization. For CMS in benzene at room temperature the percentage of the *cis* and *trans* isomers in the photostationary state and the quantum yields $\phi_{t\to c}$ and $\phi_{c\to t}$ are shown in Fig. 1 as functions of the ferrocene (azulene) concentration [Q]. $\phi_{t\to c}$ decreases slightly on increasing [Q] whereas $\phi_{c\to t}$ is constant up to [Q] values of about 10^{-1} M. On increasing [Q] the position of the photostationary state is therefore shifted to the *trans* side. Under the assumption that only the *trans* configuration $^1t^*$ of the first excited singlet state is affected by the quencher, $\phi_{t\to c}$ is given by eqn. (2), where τ_S is the fluorescence lifetime and k_q is the quenching rate constant. Linear dependences and the same slope/intercept ratios are expected for plots of $\phi_{c\to t}/\phi_{t\to c}$ and $([t]/[c])_s$ *versus* [Q] using eqns. (1) and (2).

$$\frac{\phi^0_{t\to c}}{\phi_{t\to c}} = 1 + \tau_S k_q [Q] \qquad (2)$$

$\phi_{c\to t}/\phi_{t\to c}$ and $([t]/[c])_s$ were found to be linearly dependent on [Q]. Values for slope/intercept r of the latter plot are given in Table 3 for various cases; they range between 10 and 30 M^{-1} whereas those for the corresponding nitrostilbenes are more than an order of magnitude larger. Replacing ferrocene by azulene gives similar results (Table 3). This experiment was carried out with CMS and CDMAS since much higher azulene concentrations

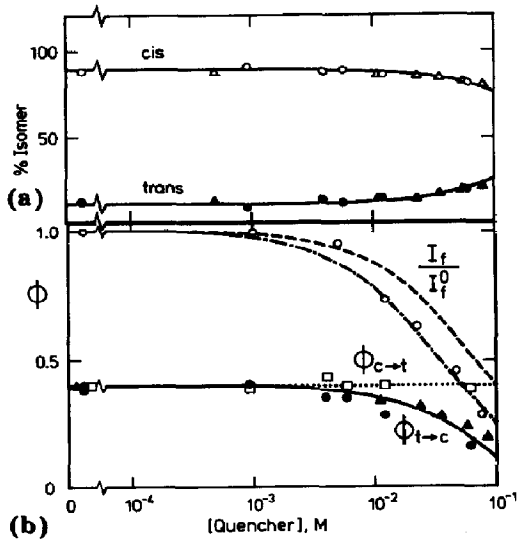

Fig. 1. The *cis–trans* photoisomerization of CMS in benzene as a function of the concentration of ferrocene (○, ●, □) or azulene (△, ▲) in the absence of oxygen at 25 °C and with λ_{irr} = 366 nm. (a) The percentage of *cis* and *trans* isomers in the photostationary state *vs.* [Q]. (b) The quantum yields of direct *cis*⇄*trans* photoisomerization and the relative fluorescence intensity (○) *vs.* [Q]. The curves were calculated using eqns. (1) - (3) and K_S = 15 M^{-1} (——, – – –) and K_S = 30 M^{-1} (– · – · –).

could be used on irradiation at 366 nm than at 313 nm because of the spectral window of azulene in the 400 nm region.

However, quenching by oxygen does not significantly affect the position of the photostationary state. No discernible changes of $([t]/[c])_s$ were found for CS, DCS and CMS when the samples were saturated either with argon or with oxygen. Oxygen at pressures of up to 50 bar (corresponding to oxygen concentrations of about 0.5 M) in chloroform only slightly changes $([t]/[c])_s$ (Table 1).

3.1.2. Temperature dependence of $\phi_{t\to c}$

$\phi_{c\to t}$, $\phi_{t\to c}$ and $([t]/[c])_s$ were measured as functions of temperature in ethanol and glycerol triacetate (GT). Semilogarithmic plots of $\phi_{t\to c}$ *versus* T^{-1} are shown in Fig. 2 for DCS and CMS in ethanol and in Fig. 3 for CS, DCS and CMS in GT. On decreasing the temperature $\phi_{t\to c}$ decreases whereas $\phi_{c\to t}$ remains almost constant. In GT at −75 °C, $\phi_{t\to c}$ is about 0.1 for CS and CMS but is much smaller (approximately 0.01) for DCS. For DCS, compared with CMS (Fig. 3) and CS (see Fig. 9), a larger decrease of $\phi_{t\to c}$ with decreasing temperature was also found in ethanol. In most cases examined $\phi_{c\to t}$ is noticeably reduced only at very high viscosities, similar to the case of various other stilbenes [8, 26 - 28].

TABLE 3

Effect of ferrocene on fluorescence (Stern–Volmer constant K_S) and on photostationary *trans/cis* ratios (slope/intercept r) for cyanostilbenes and nitrostilbenes in solution at room temperature[a]

Compound	*Solvent*[b]	$R \equiv CN$		$R \equiv NO_2$[c]	
		$K_S\,(M^{-1})$	$r\,(M^{-1})$	$K_S\,(M^{-1})$	$r\,(M^{-1})$
4-R-stilbene	Benzene	≤50	12	–[d]	630
	Methanol	≤30	10	–[d]	1150
4,4'-Di-R-stilbene	Benzene	≤30	30	–[d]	1850
	Methanol	≤25	15	–[d]	2080
4-R-4'-methoxystilbene	Cyclohexane	20		12	470
	Benzene	≤30 (≤30)[e]	12 (15)[e]	30	1100
	Methanol	≤35	10 (12)[e]	30	3800
	Dimethylformamide		10	<80	2050
4-R-4'-dimethylaminostilbene	Cyclohexane	≤30	20		
	Benzene	≤30	21 (19)[e]		
	Methanol		25		
	Dimethylformamide	≤25	15		

[a] For CS and DCS λ_{irr} = 313 nm; for the other silbenes λ_{irr} = 366 nm.
[b] Deoxygenated solutions for photoisomerization measurements; air-saturated solutions for fluorescence measurements.
[c] Values for the nitrostilbenes were taken from refs. 6, 10 and 11.
[d] The values for ϕ_f ($< 10^{-3}$) were too small to permit quenching measurements.
[e] The values in parentheses were obtained by replacing ferrocene with azulene.

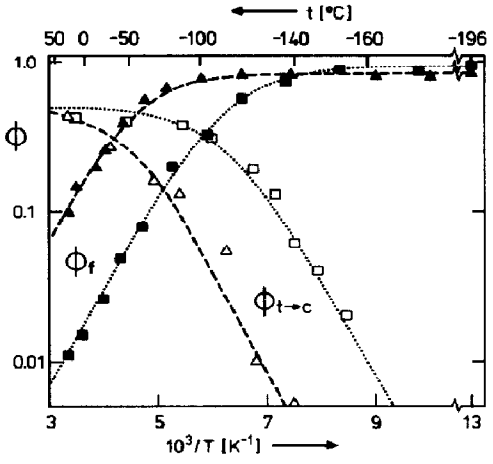

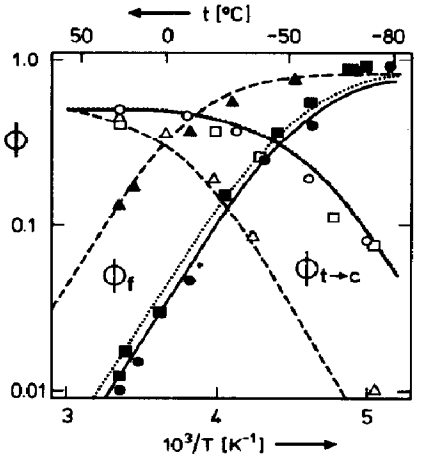

Fig. 2. ϕ_f (▲, ■) and $\phi_{t\to c}$ (△, □) *vs.* T^{-1} for *trans*-cyanostilbenes in ethanol: DCS, ▲, △, – – –, λ_{irr} = 313 nm; CMS, ■, □, . . ., λ_{irr} = 366 nm. The curves were calculated using eqns. (4) and (9), β = 0.5 and data from Table 5.

Fig. 3. ϕ_f (●, ▲, ■) and $\phi_{t\to c}$ (○, △, □) *vs.* T^{-1} for *trans*-cyanostilbenes in GT: CS, ●, ○, —, λ_{irr} = 313 nm; DCS, ▲, △, - - -, λ_{irr} = 313 nm; CMS, ■, □, . . ., λ_{irr} = 366 nm. The curves were calculated using eqns. (4) and (9), β = 0.5 and data from Table 5.

3.2. Fluorescence measurements

3.2.1. Fluorescence spectra

Trans-cyanostilbenes show fluorescence emission at room temperature in contrast with the corresponding *cis* isomers. The fluorescence emission and excitation spectra of *trans*-CS in ethanol at room temperature and at —196 °C are shown in Fig. 4 together with the absorption spectra. The absorption and emission spectra show a typical mirror image relationship. The similarity of the absorption and excitation spectra indicates that emission occurs only from the lowest excited singlet state. The absorption and fluorescence spectra of *trans*-CS are similar to the corresponding spectra of *trans*-stilbene (see for example refs. 12, 26 and 27).

Maxima of the absorption, the fluorescence excitation and the fluorescence emission spectra of the *trans*-cyanostilbenes are listed in Table 4. The absorption and fluorescence excitation spectra are red shifted in the series CS, DCS, CMS, CDMAS from approximately 320 to about 390 nm. The absorption maxima are almost independent of solvent properties. Solvent polarity, however, has some influence on the position of the fluorescence emission spectra of CMS and CDMAS. The fluorescence emission maxima range from 370 nm for *trans*-CS to 420 - 520 nm for *trans*-CDMAS. The effect of solvent properties on the emission maxima of CDMAS has been studied earlier by Lippert and coworkers [29, 30].

On going to low temperatures the absorption spectrum and the fluorescence excitation and fluorescence emission spectra become more structured (see Fig. 4(b)) because the vibrational and torsional modes are hindered by

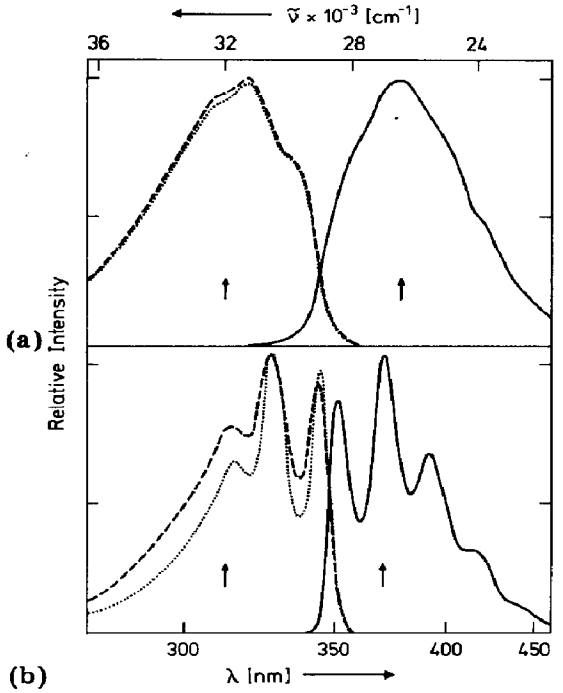

Fig. 4. Absorption spectrum (. . .), fluorescence excitation spectrum (- - -), $\lambda_{em} \approx 372$ nm) and corrected emission spectrum (——, $\lambda_{exc} = 313$ nm) of *trans*-CS in ethanol (a) at 25 °C and (b) at −196 °C.

the increasing viscosity. Similar spectra were therefore obtained in GT at −75 °C and in a mixture (1:1 by volume) of methylcyclohexane and isohexane (MCH–IH), in 2-methyltetrahydrofuran (MTHF) and in ethanol at −196 °C. The fluorescence and absorption spectra show a pronounced structure for CS and DCS whereas almost no structure was found for CDMAS (Table 4).

From the emission spectra no indication of phosphorescence was found for CS and DCS at −196 °C in the wavelength region 450 - 700 nm. Fluorescence spectra for CS and DCS in ethanol at −196 °C obtained by laser flash photolysis, *i.e.* following the laser pulse (⩽ 10 ns), were found to be similar to the aforementioned time-independent spectra. In agreement with corresponding results for stilbene (see refs. 13, 31 - 33) it is suggested that 4-cyanostilbenes show no (or only very weak) phosphorescence.

3.2.2. Fluorescence quenching measurements

Fluorescence quenching measurements were performed with ferrocene or azulene as quenchers. In the wavelength region where the quenchers absorb only slightly, the fluorescence intensity I_f decreases on increasing [Q] (Fig. 1). In the simplest case fluorescence quenching is given by the Stern–Volmer equation eqn. (3):

$$\frac{I_f^0}{I_f} = 1 + K_S[Q] \qquad (3)$$

TABLE 4

Maxima of absorption, fluorescence excitation and fluorescence emission spectra of *trans*-cyanostilbenes

Compound	*Solvent*	*t* (°C)	*Maxima* (nm)		
			Absorption	*Excitation*[a]	*Emission*[b]
CS	MCH–IH	25	(308)[c], 321, (337)	316	345, 362, 382
		−196		329, 344	350, 370, 390, (412)
	Ethanol	25	(306), 320, (336)	319, 335	(350), 374
		−196	(313), 326, 343	328, 345	350, 370, 391, (410)
	GT	25	(307), 321, (337)	327, (339)	352, 370
		−75			352, 370, 390, (412)
DCS	MCH–IH	25	313, 326, (342)	(310), 324, (340)	353, 368, 388
	Ethanol	25	(314), 326, 343	324, (340)	356, 377, (393)
		−196	315, 331, 348	320, 333, 351	354, 374, 397, (420)
	GT	25	315, 327, 344	(316), 331, 347	356, 374, 396
CMS	MCH–IH	25	(325), 340, (357)	338	(375), 395, 412
		−196		348, 363	395, 421, 446
	Ethanol	25	336	340, (360)	415
		−196	(333), 348, 364	351, 366	381, 400, (420)
	GT	25	340		407
CDMAS	MCH–IH	25	381	380	417, 440, (470)
	Ethanol	25	385	400	522
		−196	≈405		454, 473
	GT	25	388	392	495

[a]Emission measured approximately at the maxima of the fluorescence spectra.
[b]For CS and DCS λ_{exc} = 313 nm; for the other stilbenes λ_{exc} = 366 nm.
[c]Values in parentheses refer to shoulders in the spectra.

Linear Stern–Volmer plots were found for various cases using quencher concentrations of up to 0.05 M. Stern–Volmer constants ($K_S = \tau_S k_q$) obtained from the *trans*-cyanostilbenes in several solvents are listed in Table 3. At higher quencher concentrations the fraction of fluorescence from the stilbenes which is absorbed by the quencher may be quite significant [15]. Because of this effect the uncorrected values for K_S may be overestimated (see Fig. 1).

In contrast with the case of ferrocene (or azulene) no independent method was available for measuring the effect of oxygen on $^1t^*$ since fluorescence quenching could not be carried out using the high pressure absorption cell. Apparently quenching of $^1t^*$ by oxygen is less efficient than quenching by ferrocene. Similar results have been reported for the stilbene–azulene system [13 - 16].

3.2.3. Temperature dependence of ϕ_f

Values for ϕ_f of the *trans*-cyanostilbenes in several solvents at room temperature are listed in Table 5. ϕ_f is about 0.01 for CS and CMS but is significantly larger (0.1) for DCS. The temperature dependence of ϕ_f was measured in MCH–IH, MTHF, ethanol and GT. Semilogarithmic plots of ϕ_f *versus* T^{-1} in ethanol are shown in Fig. 2. On decreasing the temperature ϕ_f increases and reaches a value close to unity below about −140 °C. In GT as solvent ϕ_f increases at much higher temperatures and reaches a maximum value ϕ_f^0 at −80 °C (Fig. 3). For all the cyanostilbenes studied the ϕ_f^0 values are close to unity in the solvents used (Table 5).

The temperature dependence of ϕ_f for the cyanostilbenes is very similar to that of stilbene, which has been studied intensively by several workers [12 - 18, 26 - 28, 31]. Analogous to this case, competition between fluorescence emission, a non-activated radiationless deactivation step and an activated radiationless deactivation step was assumed. The temperature-dependent step is assigned to twisting in the excited singlet state from the *trans* $^1t^*$ configuration to the perpendicular $^1p^*$ configuration and the radiationless temperature-independent step may be intersystem crossing or internal conversion [4]. The temperature dependence of ϕ_f was analysed using eqn. (4):

$$\ln(\phi_f^{-1} - \kappa) = \ln\left(\frac{A}{k_f}\right) - \frac{E_a}{RT} \tag{4}$$

Here $\kappa = 1 + k_0/k_f$, where k_f and k_0 are the rate constants of fluorescence and of the non-activated deactivation step from $^1t^*$ respectively; E_a is the activation energy and A is the pre-exponential factor for the activated twisting step $^1t^* \rightarrow {}^1p^*$. Values for κ, A/k_f and E_a were obtained from linear plots of $\ln(\phi_f^{-1} - \kappa)$ *versus* T^{-1} (Table 5). For CS, CMS and CDMAS in liquid solutions E_a values of about 13 kJ mol^{-1} and A factors of the order of 10^{12} - 10^{13} s^{-1} were obtained. For DCS a similar activation energy but a smaller A factor were derived. Because of the smaller rate constant of the activated step, larger ϕ_f values at higher temperatures and smaller $\phi_{t\rightarrow c}$ values at

TABLE 5

Quantum yields of fluorescence of *trans*-cyanostilbenes and parameters obtained from the temperature dependence of ϕ_f[a]

Compound	*Solvent*	ϕ_f[b]	ϕ_f^0[b]	κ[c]	E_a (kJ mol^{-1})	A/k_f
CS	MCH–IH	0.01	0.9	1.1		
	Ethanol	0.007	0.9	1.1	13	3×10^4
	GT	0.010	0.8	1.2	29	1×10^7
DCS	MCH–IH	0.15				
	Ethanol	0.10	0.8	1.2	13.5	2×10^3
	GT	0.13	0.8	1.2	31	1.6×10^6
CMS	MCH–IH	0.01	0.9	1.1	13	2×10^4
	Toluene[d]	0.013			12	7.8×10^3
	MTHF	0.012	0.9	1.1	12.5	2×10^4
	Ethanol	0.011	0.95	1.05	12.5	1.3×10^4
	Methanol[d]	0.012			13	1.7×10^4
	Dimethyl-formamide[d]	0.017			17	4.6×10^4
	GT	0.012	0.9	1.1	28	5×10^6
CDMAS	Ethanol	0.04	0.9	1.1	15	1×10^4
	GT	0.05	0.9	1.1	33	1.5×10^7

[a]For CS and DCS λ_{exc} = 313 nm; for the other stilbenes λ_{exc} = 366 nm.
[b]ϕ_f refers to 25 °C; ϕ_f^0 refers to −80 °C for GT and to −196 °C for MCH–IH, MTHF and ethanol.
[c]$\kappa = 1 + k_0/k_f$.
[d]Values taken from ref. 4.

lower temperatures were found for DCS. In more viscous solvents considerably higher A factors and activation energies were found for all the cyanostilbenes studied. These higher E_a values and A factors are due to temperature-dependent and viscosity-dependent activation barriers against twisting in the excited singlet state (see refs. 12 and 18).

Rate constants for the decay of $^1t^*$ are given in Table 6. Using these data the maximum quantum yield ϕ_{isc} for intersystem crossing and the fluorescence lifetime at room temperature and at −196 °C were calculated. At room temperature ϕ_{isc} is very small (approximately 10^{-3}) for CS and CMS and the τ_S values range between 20 and 200 ps. These short fluorescence lifetimes could not be measured with our equipment because of the limited time resolution of the fluorimeter (about 1.0 ns). However, results from the τ_S measurements at −196 °C agree with calculated values assuming the condition $\tau_S^0 = \phi_f^0/k_f$ (Table 6).

3.3. *Sensitized* cis–trans *photoisomerization*

Sensitized *cis–trans* isomerization was performed for CMS in benzene at room temperature. A plot of the *cis/trans* ratio $([c]/[t])_{sens}$ in the photostationary state as a function of the triplet energy E_T is shown in Fig. 5 ("Saltiel plot"). With increasing E_T, $([c]/[t])_{sens}$ increases, then decreases

TABLE 6

Rate constants for decay of $^1t^*$, τ_S and ϕ_{isc} for *trans*-cyanostilbenes

Compound	*Solvent*	k_f[a] ($\times 10^8\ s^{-1}$)	k_0[b] ($\times 10^8\ s^{-1}$)	$Ae^{-E_a/RT}$[c] ($\times 10^8\ s^{-1}$)	τ_S[d] (ns)	τ_S^0 (ns)	ϕ_{isc}[e]	ϕ_{isc}^0
CS	Ethanol	5.0	0.5	790	0.01	1.8(1.5)[f]	0.006	0.09
	GT	5.1	1.0	410	0.02	1.6(1.5)	0.002	0.16
DCS	Ethanol	5.0	1.0	43	0.20	1.7(1.5)	0.022	0.17
	GT	4.9	1.0	30	0.28	1.7(1.5)	0.028	0.17
CMS	Ethanol	4.3	0.3	340	0.03	2.2(1.5)	0.001	0.07
	GT	4.2	0.4	250	0.04	2.2(1.7)	0.002	0.09
CDMAS	Ethanol	3.7	0.5	96	0.1	2.4(2.0)	0.005	0.12
	GT	3.6	0.5	100	0.1	2.4(2.1)	0.005	0.12

[a]Obtained from absorption spectra, see ref. 4.
[b]Calculated from k_f and ϕ_f^0.
[c]Values refer to 25 °C and were calculated using data from Table 5.
[d]Values refer to 25 °C and were calculated using data from Table 5 and $\tau_S = \phi_f/k_f$.
[e]Values refer to 25 °C and were calculated using data from Table 5 and $\phi_{isc} = \tau_S k_0$.
[f]Values in parentheses were measured at −196 °C.

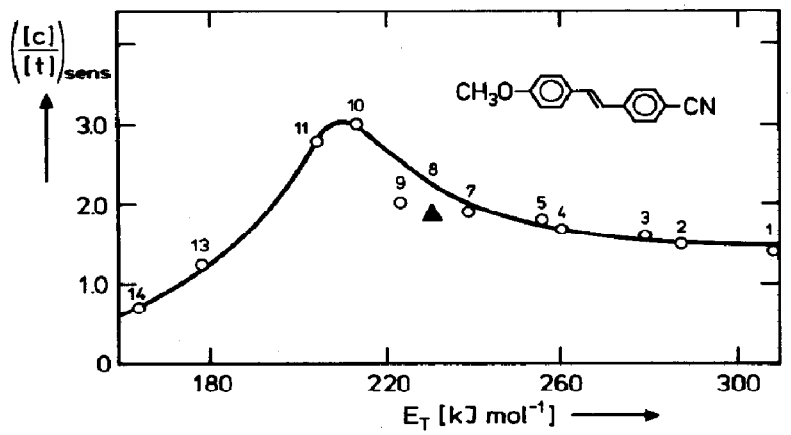

Fig. 5. Photostationary *cis/trans* ratios under sensitized excitation conditions as a function of the triplet energy of sensitizers ("Saltiel plot") for CMS in benzene at 25 °C. The sensitizers are the same as those indicated in Fig. 6 (except for 1, acetophenone; 4, phenanthrene; 14, azulene); ○, λ_{irr} = 254 nm; ▲, λ_{irr} = 417 nm.

between 215 and 240 kJ mol^{-1} and finally reaches a constant value. From this value the fraction α of triplet which decays to the *trans* ground state ^{1}t was derived. The value $\alpha = 0.42$ for CMS in benzene [7] is similar to those obtained from the corresponding Saltiel plots for CDMAS, for several nitrostilbenes [7] and for stilbene [13, 16].

In order to determine the triplet lifetime of CMS in solution at room temperature, naphthalene-sensitized photoisomerization was performed in the presence of ferrocene. On increasing [Q] the position of the photostationary state was shifted to the *trans* side and the rate of isomerization was reduced owing to the absorption by ferrocene at λ_{irr} = 254 nm. Assuming that the rates of triplet energy transfer from the sensitizer to the *trans* and *cis* isomers are equal and that there is no energy wastage, the effect of ferrocene on the triplet state of CMS is given by eqn. (5) [7, 13, 14]:

$$\left(\frac{[t]}{[c]}\right)_{sens} = \frac{\alpha}{1-\alpha}\left(1 + \frac{\tau_T k_q}{\alpha}[Q]\right) \qquad (5)$$

Plots of $([t]/[c])_{sens}$ were found to be linearly dependent on [Q] (up to [Q] = 1×10^{-2} M). Values for slope/intercept of 45 and 65 M^{-1} were obtained in benzene and methanol respectively.

The rate constant k_q for quenching of the triplet states of CMS by ferrocene is not known. For quenching of the stilbene triplets by azulene a value well below the diffusion-controlled limit has been reported by Saltiel and coworkers [14, 34]. For the NMS–ferrocene system values for k_q of 5.5×10^9 and 9.9×10^9 M^{-1} s^{-1} have been found for benzene and methanol respectively [10]. Assuming these k_q values for CMS a triplet lifetime at room temperature of 3.4 and 2.8 ns in benzene and methanol respectively was calculated using eqn. (5) and $\alpha = 0.42$.

3.4. Laser flash photolysis

In previous work the detection of a transient intermediate of CMS by nanosecond laser flash photolysis was not successful [1]. However, in the highly viscous solvent GT at low temperatures a transient, which was tentatively assigned to a triplet state, has been observed recently for *trans*-CMS [8]. In liquid solution at room temperature no transient absorption having a lifetime longer than 10 ns was found in the range from about 370 to 800 nm for CS, DCS and CMS. However, for *trans*-CS and *trans*-DCS in several solvents (*e.g.* MTHF, ethanol and GT) a transient absorption signal was observed at approximately 590 nm (halfwidth about 50 nm). For *trans*-CMS and *trans*-CDMAS no transient absorption could be measured in the 10 ns region because of the fluorescence emission between 400 and 650 nm. Since decay of the transient is faster than the duration of the laser pulse (about 10 ns) no lifetime could be measured with nanosecond laser flash photolysis. The short-lived transient is assigned to $S_1 \rightarrow S_n$ absorption of the $^1t^*$ state. This is confirmed by the result that approximately the same absorption spectrum and a lifetime of less than 10 ns were found for *trans*-CS and *trans*-DCS in ethanol at low temperatures (−100 to −180 °C).

It is interesting to note that the absorbance of the transition $S_1 \rightarrow S_n$ is much greater than that of the transition $T_1 \rightarrow T_n$ (see Section 3.4.2) at low temperatures. A similar $S_1 \rightarrow S_n$ absorption spectrum and a fluorescence lifetime at room temperature of about 100 ps has been reported recently for stilbene [35].

3.4.1. Energy transfer

In order to study further the role of triplet states of cyanostilbenes (in liquid solutions) in the *cis–trans* isomerization, energy transfer experiments were performed. However, no transient with a lifetime of longer than 50 ns was found between 380 and 800 nm for CS and CMS in benzene at room temperature using high energy triplet sensitizers (*e.g.* naphthalene, benzophenone or xanthone).

However, the triplet states of these compounds are quenched at approximately diffusion-controlled rates. Linear dependences of the rate constant τ^{-1} for triplet decay as a function of the concentration of CMS (eqn. (6)) were found:

$$\tau^{-1}/\tau_0{}^{-1} = 1 + \tau_0 k_q [\text{CMS}] \qquad (6)$$

A plot of the bimolecular quenching rate constant k_q as a function of E_T ("Herkstroeter plot" [36]) is shown in Fig. 6. From this plot a triplet energy for *trans*-CMS of approximately 208 kJ mol^{-1} was obtained. A very similar triplet energy of 215 kJ mol^{-1} has been reported for *trans*-stilbene [13, 14, 36].

3.4.2. Triplet absorption spectrum

On going to low temperatures and correspondingly high viscosities, transients which are assigned to triplet states (see Section 4) were found for

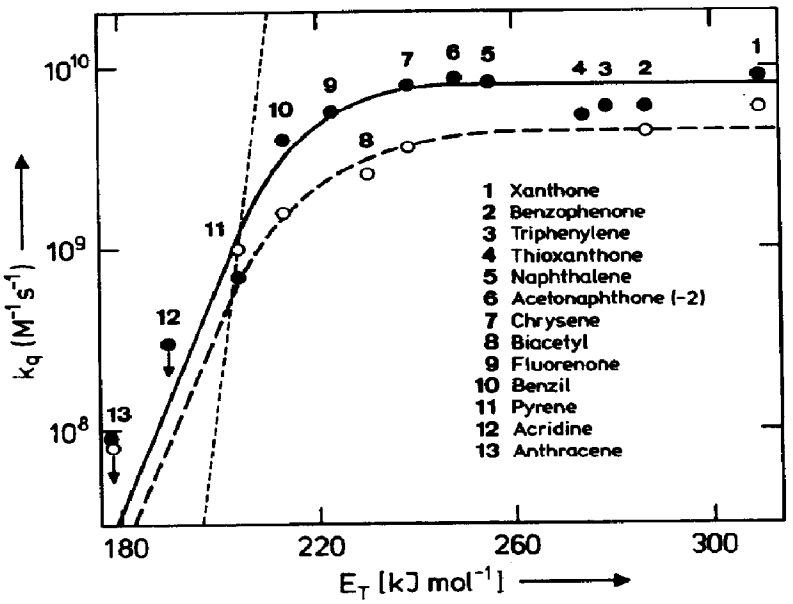

Fig. 6. Rate constants for quenching of triplet states of sensitizers by *trans*-CMS in benzene (○, λ_{exc} = 353 nm) and/or methanol (●, λ_{exc} = 265 nm) as a function of E_T ("Herkstroeter plot") at 25 °C. For acridine (12) and anthracene (13) k_q values are upper limits due to too low a concentration of CMS. The broken straight line corresponds to the condition $\Delta \log k_q = -\Delta E_T/2.3RT$, see ref. 36.

the *trans*-cyanostilbenes. The triplet–triplet absorption spectra of CS, DCS and CMS in GT at —75 °C are shown in Fig. 7. Absorption maxima at 405, 410 and 450 nm were found for CS, DCS and CMS respectively. Similar triplet–triplet absorption spectra were observed in glycerol at —75 °C, in MTHF and ethanol below approximately —140 °C and in PMMA matrices at

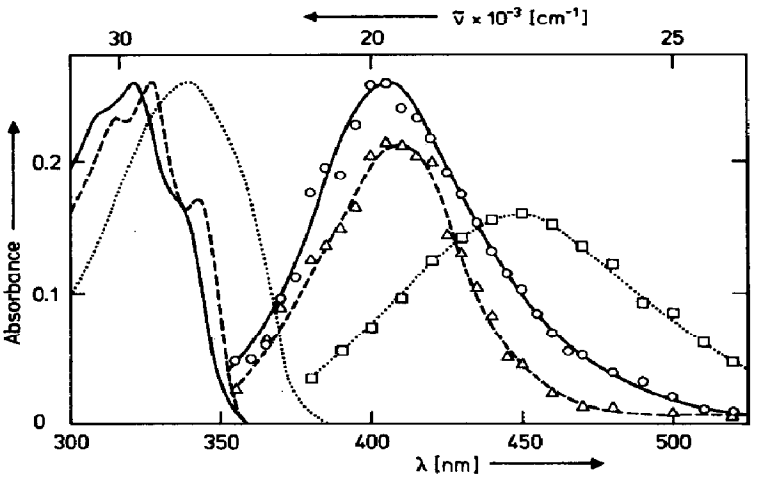

Fig. 7. Triplet–triplet absorption spectra of *trans*-cyanostilbenes in GT at —75 °C (λ_{exc} = 353 nm) and ground state absorption spectra in GT at room temperature: ○, ——, CS; △, - - -, DCS; □, . . ., CMS.

room temperature (Table 7). For *trans*-CDMAS only a very weak transient absorption was observed between 460 and 700 nm in GT and MTHF at high viscosities.

3.4.3. Triplet yield

For CS, DCS and CMS in GT the absorbance of the triplet state *versus* T^{-1} is shown in Fig. 8. The absorbance of the triplet is first observed at about −30 °C and increases up to a constant value at about −70 °C. Assuming that the extinction coefficient for triplet–triplet absorption is temperature independent the absorbance is proportional to the yield ϕ_T of triplet formation. Analogous to the case of halogenated stilbenes [18] competition between temperature-independent triplet formation (k_0') and an activated step (A' exp ($-E_a'/RT$)) was assumed. The latter step may be twisting either in the excited singlet state or in a higher triplet state (see Section 4). The activation energy E_a' and the pre-exponential factor A'/k_0' were calculated from the temperature dependence of the triplet yield using eqn. (7) and assuming $\phi_{isc}^0 = 1 - \phi_f^0$. Values for E_a' and A'/k_0' are listed in Table 8.

$$\ln\left(\frac{\phi_{isc}^0}{\phi_T} - 1\right) = \ln\left(\frac{A'}{k_0'}\right) - \frac{E_a'}{RT} \tag{7}$$

3.4.4. Triplet lifetime

Decay of the triplet was found to be first order. The temperature dependence of the first order decay rate constant $k_{obsd} = \tau_T^{-1}$ is shown in Fig. 8 for *trans* isomers of CS, DCS and CMS in GT. Below the maximum temperature t_m, where the triplet is observed, $\log \tau_T^{-1}$ decreases linearly as a function of T^{-1} and reaches a constant value at t_0 (Fig. 8). Values for t_m, t_0 and for the decay rate constants at t_m and the lowest temperatures ($< t_0$) accessible (k_m and k_0 respectively) are listed in Table 7.

Analogous to the case of halogenated stilbenes [18] an Arrhenius behaviour (A_τ exp ($-E_\tau/RT$)) was assumed for the viscosity-dependent triplet decay rate constant. The temperature dependence of τ_T^{-1} below t_m was calculated using eqn. (8):

$$\ln\left(\frac{1}{k_0 \tau_T} - 1\right) = \ln\left(\frac{A_\tau}{k_0}\right) - \frac{E_\tau}{RT} \tag{8}$$

Values for A_τ and E_τ are listed in Table 8. The activated step reflects the effects of temperature and viscosity on twisting in the lowest triplet state. E_τ represents the sum of at least two activation barriers and A_τ is the product of at least two A factors. Values for A_τ and E_τ are exceedingly large but are in the same range as those for stilbene [18]. For *trans*-CS in ethanol the temperature dependences of ϕ_f, $\phi_{t\to c}$, ϕ_T and τ_T^{-1} are shown in Fig. 9. The curves for ϕ_f and $\phi_{t\to c}$ were calculated using data from Table 5 and assuming the same activation barrier for both processes (see Section 4). ϕ_T and τ_T^{-1} reach constant values at temperatures where $\phi_{t\to c}$ is very small.

TABLE 7

Triplet–triplet absorption maxima and triplet decay rate constants at t_m[a] and t_0[b] for *trans*-cyanostilbenes

Compound	*Solvent*[c]	λ_{max} (nm)	λ_{exc} (nm)	t_m[a] (°C)	$k_m \times 10^{-5}$ (s^{-1})	t_0[b] (°C)	$k_0 \times 10^{-2}$[d] (s^{-1})
CS	MTHF	405 (−175)[e]	265	−146	6	−169	1
	Ethanol	400 (−155, −170)	265, 353	−135	6	−163	0.6
	GT	405 (−75)	353	−34	10	−63	1
	PMMA	395 (+25)	353				
DCS	MTHF	415 (−140, −160)	265	−139	10	−174	0.8
	Ethanol	410 (−138, −170)	353	−135	4	−163	0.8
	GT	410 (−75)	353	−30	10	−59	1.5
	PMMA	405 (+25)					
CMS	MTHF	410, 490 (−130, −165)	265	−130	3	−167	1
	Ethanol	420, 480 (−135, −160)	353	−141	2	−160	0.8
	GT	450 (−50, −76)	353	−35	5	−67	1
	Glycerol	420, 490 (−75)	353				
	PMMA	430 (+25)	353				
CDMAS	MTHF	460, ≈700 (−140)	353				
	GT	460 - 700 (−75)	353				

[a] t_m specifies the highest temperature at which triplet–triplet absorption was still measurable.

[b] t_0 specifies the temperature where the straight lines of the temperature-dependent and temperature-independent parts of $\log \tau_T^{-1}$ *vs.* T^{-1} cross.

[c] Deoxygenated solutions.

[d] Values refer to $t < t_0$.

[e] Values in parentheses refer to the temperature (°C) at which the triplet–triplet absorption spectrum was measured.

TABLE 8

Activation energies and A factors obtained from the temperature dependence of formation and decay of the observed triplet state

Compound	*Solvent*	E_a'[a] (kJ mol^{-1})	A'/k_0'[a]	E_τ[b] (kJ mol^{-1})	A_τ[b] (s^{-1})
CS	MTHF	25	2×10^{10}	40	1×10^{22}
	Ethanol	28	1×10^{11}	42	5×10^{21}
	GT	67	2×10^{15}	130	2×10^{34}
DCS	MTHF	25	3×10^{9}	46	2×10^{25}
	Ethanol	28	5×10^{10}	38	8×10^{19}
	GT	71	3×10^{15}	126	1×10^{34}
CMS	MTHF	25	2×10^{8}	31	1×10^{17}
	Ethanol	28	3×10^{10}	43	2×10^{22}
	GT	67	2×10^{15}	126	2×10^{33}

[a]Obtained from the temperature dependence of ϕ_T using eqn. (7).
[b]Obtained from the temperature dependence of τ_T using eqn. (8) and values for k_0 from Table 7.

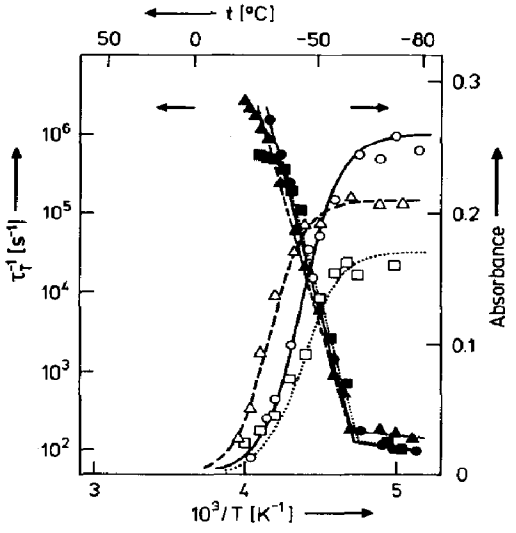

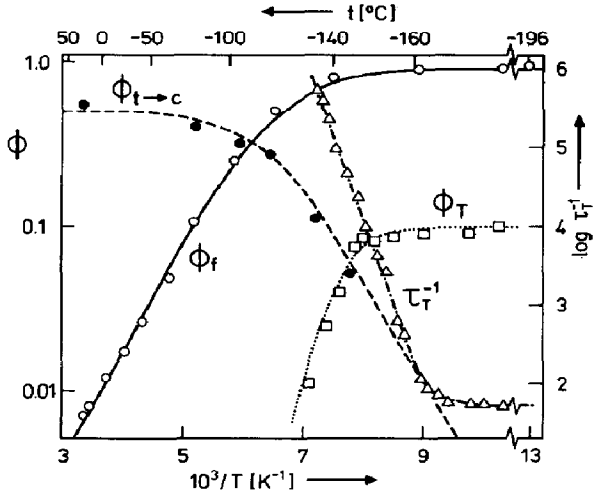

Fig. 8. Absorbances from triplet absorption (○, △, □) and reciprocal triplet lifetimes in the absence of oxygen (●, ▲, ■) *vs.* T^{-1} for *trans*-cyanostilbenes in GT (λ_{exc} = 353 nm): ●, ○, ——, CS; ▲, △, - - -, DCS; ■, □, · · ·, CMS. The curves for the absorbance were calculated using eqn. (7) and data from Table 8.

Fig. 9. ϕ_f, $\phi_{t\rightarrow c}$, ϕ_T and τ_T^{-1} (s^{-1}) *vs.* T^{-1} for *trans*-CS in ethanol. ϕ_T was obtained from the absorbance assuming $\phi_T^{max} = 1 - \phi_f^0$. The curves were calculated using eqns. (4), (9), (7) and (8) for ϕ_f, $\phi_{t\rightarrow c}$, ϕ_T and τ_T^{-1} respectively, β = 0.5 and data from Tables 5 - 8.

4. Discussion

4.1. Singlet states

From the experimental results for the cyanostilbenes examined, a reaction scheme for *cis* $\rightleftarrows$ *trans* photoisomerization may be deduced on the basis of the following results.

Ferrocene (or azulene) quenches the fluorescence and the *trans*→*cis* photoisomerization of the cyanostilbenes (Fig. 1). If in *trans*$\rightleftarrows$*cis* isomerization the $^1t^*$ state is the only state which is quenched by ferrocene, the same Stern–Volmer constants $\tau_S k_q$ are predicted from quenching measurements of *trans*→*cis* isomerization and fluorescence, *i.e.* the same values for slope/intercept are predicted from plots of I_f^0/I_f, $\phi_{t\to c}^0/\phi_{t\to c}$, $\phi_{c\to t}/\phi_{t\to c}$ and $([t]/[c])_s$ *versus* [Q] (see refs. 6 and 16). Equal quenching constants were found, within experimental error, from Stern–Volmer plots of fluorescence and from plots of photostationary *trans*/*cis* ratios *versus* [Q], *i.e.* $r = K_S$ (see Table 3). From these results it is suggested that the *trans*→*cis* photoisomerization of the cyanostilbenes occurs via a singlet pathway.

Analysis of the temperature dependence of ϕ_t shows that an activated deactivation step is the main competitor to fluorescence. The A factor of 10^{12} - 10^{13} s^{-1} in solvents with low viscosity (*e.g.* toluene, MTHF, ethanol and dimethylformamide) is in agreement with the assumption that $^1t^*$ decays mainly by twisting in the first excited singlet state. Larger A factors in GT can reasonably be explained by an additional viscosity-dependent barrier which must be overcome during the twisting step $^1t^* \rightarrow {}^1p^*$ (see refs. 12 and 18).

If twisting in the excited singlet state is the only activated process in *trans*→*cis* photoisomerization, identical activation energies are expected both for deactivation of $^1t^*$ and for *trans*→*cis* isomerization [18]. This is indeed the case. The temperature dependences of $\phi_{t\to c}$ in ethanol and GT agree well with calculated curves using eqn. (9) and data from fluorescence measure-

$$\phi_{t\to c} = (1-\beta)\frac{A e^{-E_a/RT}}{k_t + k_0 + A e^{-E_a/RT}} \qquad (9)$$

For the fraction β of $^1p^*$ which decays to ^1t via the twisted ground state ^1p, temperature independence and a value of 0.5 was assumed throughout. Values for β of 0.46 for stilbene [16] and of 0.3 for NMS in cyclohexane [6] have been reported.

The results presented strongly support the singlet pathway for *trans*→*cis* (eqn. (10a)) and *cis*→*trans* (eqn. (10b)) photoisomerization in liquid solutions as presented in Scheme 1. For stilbene these singlet pathways have been well established by Saltiel and coworkers [12 - 16, 32].

$$^1t \xrightarrow{h\nu} {}^1t^* \longrightarrow {}^1p^* \longrightarrow {}^1p \longrightarrow (1-\beta)\,{}^1c \qquad (10a)$$

$$^1c \xrightarrow{h\nu} {}^1c^* \longrightarrow {}^1p^* \longrightarrow {}^1p \longrightarrow \beta\,{}^1t \qquad (10b)$$

Scheme 1.

Substantial values for $\phi_{t\rightarrow c}$ and $\phi_{c\rightarrow t}$ were found for the 4-cyanostilbenes in liquid solution at room temperature (see Table 2). This shows that *cis*⇄*trans* photoisomerization is the major photochemical process at low stilbene concentrations. Formation of DHP from *cis*-cyanostilbenes is considered to be less important than it is for stilbene [20, 37]. However, involvement of excited singlet and triplet states of DHP and subsequent formation of $^3p^*$, as suggested by Saltiel *et al.* [16] for 4-bromostilbene, cannot be excluded for the cyanostilbenes. Fluorescence emission from the *cis* isomer at low temperatures was not studied in this work. Since $\phi_{c\rightarrow t}$ decreases at very high viscosities a deactivation pathway $^1c^* \rightarrow {}^1c$, not leading to ^1t and which is either radiative or radiationless, is suggested.

4.2. Triplet states

The fact that no triplet intermediate was found in liquid solution supports the assumption of a singlet mechanism at room temperature. However, at low temperatures there is a minor radiationless deactivation pathway from $^1t^*$ which does not lead to *trans*→*cis* photoisomerization via the singlet pathway since a long-lived transient was observed for the *trans*-cyanostilbenes in highly viscous solvents. The yield and lifetime of the transient show approximately the same temperature dependence (Figs. 8 and 9) as the observed triplet state of halogenated stilbenes [17, 18]. For these stilbenes the transient has been assigned to the planar triplet state. For the *trans*-cyanostilbenes the transient is also assigned to a triplet state since the excited singlet state and a DHP triplet state are excluded. No difference in triplet–triplet absorption spectra was found between t_m, where $\phi_{t\rightarrow c}$ is still measurable, and lower temperatures where $\phi_{t\rightarrow c}$ is practically zero. If trans→*cis* isomerization is completely inhibited it is concluded that no twisting from 0 to 90° (*i.e.* no change in configuration) occurs and only *trans* states may be populated after excitation of the *trans*-cyanostilbene. Therefore the observed transient is assigned to the *trans* configuration $^3t^*$ of the lowest triplet state.

The triplet–triplet absorption spectra of 4-halogenated stilbenes [17, 18] exhibit three absorption maxima between 340 and 400 nm which are separated by a vibrational progression of about 1600 cm^{-1} [26]. However, the triplet–triplet absorption spectra of *trans*-cyanostilbenes show no pronounced structure (Fig. 7) similar to the triplet–triplet absorption spectra of 4-nitrostilbenes [1, 8]. It is likely that polar substituents lead to the disappearance of the vibrational fine structure.

At low temperatures, where the activated twisting step $^1t^* \rightarrow {}^1p^*$ is strongly reduced, the $^3t^*$ state is populated from $^1t^*$. Fluorescence measurements below —140 °C indicate the existence of a radiationless non-activated deactivation step from $^1t^*$ since ϕ_f^0 is slightly smaller than unity (see Figs. 2 and 9). Since the possibility of internal conversion ($^1t^* \rightarrow {}^1t$) cannot be excluded, $1 - \phi_f^0$ represents the maximum yield of triplet formation. The triplet yield decreases on going from —196 °C to higher temperatures (lower viscosities) and triplet absorption disappears above t_m (Figs. 8 and 9). This shows that the lowest triplet state is not formed and thus does not contribute to *trans*→*cis* photoisomerization above t_m.

Even below t_m the triplet yield is small since its maximum value is less than 0.1. At t_m *trans→cis* photoisomerization via the singlet pathway is the dominant process (see Figs. 2, 3 and 9); however, contribution from a second (minor) pathway is possible and its size may be of the order of the experimental error. For halogenated stilbenes contribution of the upper excited triplet pathway and of the lowest triplet pathway above and below t_m respectively has been found [18]. Contribution of these pathways to *trans→cis* photoisomerization may also be possible for cyanostilbenes. If $^1t^* \rightarrow {}^1p^*$ is the only activated step which competes with formation of $^3t^*$ identical activation energies are expected from the temperature dependences of ϕ_f and ϕ_T. However, a larger activation energy E_a' was obtained from triplet yield measurements (Table 8) compared with the E_a value which was obtained from fluorescence measurements (Table 5). This result suggests a minor participation of an upper excited triplet pathway [17, 18] as presented in Scheme 2. The proposed upper excited triplet state $^3t_h^*$ is possibly deactivated via $^3p^*$ but not via $^3t^*$.

$$^1t^* \longrightarrow {}^3t_h^* \longrightarrow {}^3p^* \longrightarrow {}^1p \longrightarrow \alpha\,{}^1t + (1-\alpha)\,{}^1c \qquad (11)$$

Scheme 2.

Twisting in the upper excited triplet state competes with formation of $^3t^*$. Formation of $^3t^*$ and deactivation of $^3t^*$ by twisting either to approximately 90° or to less than 90°, not leading to ^1p, is presented in Scheme 3.

$$^1t^* \longrightarrow {}^3t_h^* \longrightarrow {}^3t^* \qquad (12)$$

$$^3t^* \longrightarrow {}^3p^* \longrightarrow {}^1p \longrightarrow \alpha\,{}^1t + (1-\alpha)\,{}^1c \qquad (13)$$

$$^3t^* \longrightarrow {}^1t \quad \text{viscosity dependent} \qquad (14a)$$

$$^3t^* \longrightarrow {}^1t \quad \text{viscosity independent} \qquad (14b)$$

Scheme 3.

On decreasing the temperature between t_m and t_0 the triplet lifetime increases strongly. This is interpreted as being the result of a viscosity-dependent deactivation step, *i.e.* twisting in the lowest triplet state followed by intersystem crossing, eqn. (13) or eqn. (14a). The twisting step may contribute to $\phi_{t\rightarrow c}$ if the molecule twists to $^3p^*$ (eqn. (13)). However, since the temperature dependence of $\phi_{t\rightarrow c}$ is reasonably explained by the singlet pathway (Scheme 1) it is proposed that the viscosity-dependent deactivation step of $^3t^*$ involves twisting to an angle of less than 90° (eqn. (14a)), not leading to the *cis* ground state ^1c.

On increasing the viscosity further, twisting in the lowest triplet state is frozen out and deactivation of $^3t^*$ occurs according to eqn. (14b)). The viscosity independence and the temperature independence of τ_T below t_0, *i.e.* at temperatures where $\phi_{t\rightarrow c}$ is practically zero, has also been found for various substituted stilbenes [9, 10, 18].

4.3. Comparison between cyanostilbenes and nitrostilbenes

The difference in the *trans→cis* isomerization pathways for 4-cyanostilbenes and 4-nitrostilbenes gives rise to the following effects.

4.3.1. Cis–trans *photoisomerization*

For cyanostilbenes the position of the photostationary state and $\phi_{t\to c}$ are only slightly affected by solvent properties. However, for polar nitrostilbenes (*e.g.* NMS and NDMAS) a decrease of $\phi_{t\to c}$ and a corresponding shift of the photostationary state to the *trans* form with increasing solvent polarity have been found (see Table 1). The main reason for these effects is a radiationless decay step $^1t^* \to {}^1t$ [7] which is pronounced for polar nitrostilbenes but is apparently small for the corresponding cyanostilbenes (CMS and CDMAS).

4.3.2. Effect of quenchers

From fluorescence quenching by ferrocene or azulene similar Stern–Volmer constants were found for cyanostilbenes and nitrostilbenes. However, quenching of the *trans→cis* photoisomerization is different in both cases (Table 2). For cyanostilbenes quenching of $^1t^*$ is the only quenching process (*i.e.* $r = K_S$) whereas for nitrostilbenes quenching of $^3t^*$ is the main quenching process [2, 6]. Since τ_T is much longer than τ_S larger values for slope/intercept are found for the nitrostilbenes [10].

4.3.3. Fluorescence quantum yield

Values for ϕ_f at room temperature are moderate for cyanostilbenes but are small for several nitrostilbenes, *e.g.* NS and DNS [28]. The reason for this is the substantial value of ϕ_{isc} for the nitrostilbenes. Since the rate constant for intersystem crossing is probably temperature independent, small values for ϕ_f^0 are found for several nitrostilbenes [28, 29] ($\phi_f^0 < \phi_{isc}^0$) in contrast with the cyanostilbenes ($\phi_f^0 > \phi_{isc}^0$). Furthermore, the activation energy which is derived from the temperature dependence of ϕ_f depends on solvent polarity for NMS [4] but not for the cyanostilbenes. Involvement of ($n\pi^*$) states in the case of nitrostilbenes may account for these effects [4].

4.3.4. Triplet yield and lifetime

Because of the large difference in ϕ_{isc} the lowest triplet state is populated in solution at room temperature for nitrostilbenes but not for cyanostilbenes. The triplet lifetime ranges from 50 ns to 4 μs for 4-nitrostilbenes [1, 10] and is considered to be smaller (below 10 ns) for cyanostilbenes.

4.3.5. Effect of temperature on triplet yield and lifetime

For cyanostilbenes the triplet yield increases at high viscosities where twisting about the central double bond in higher excited singlet and triplet states is significantly reduced. For nitrostilbenes ϕ_T is mainly temperature independent and viscosity independent (*e.g.* in those cases where ϕ_f^0 is small) [8]. For nitrostilbenes in liquid solution the triplet lifetime is only slightly

temperature dependent, but increases strongly with increasing viscosity and levels off in the high viscosity range [9]. A very similar temperature dependence of τ_T^{-1} was found for cyanostilbenes in the low temperature range below t_m.

4.3.6. Effect of temperature on trans→cis *photoisomerization*

For cyanostilbenes the temperature dependence of $\phi_{t\rightarrow c}$ is determined by the activation barrier which must be overcome by the $^1t^* \rightarrow {}^1p^*$ twisting step. For nitrostilbenes in liquid solution $\phi_{t\rightarrow c}$ is essentially temperature independent. A small activation energy for NMS may be due either to competing deactivation steps from the $^3t^* \rightleftarrows {}^3p^*$ equilibrium to ^1t and ^1p or to an activation step involving higher *trans* singlet or triplet states (but not the twisted $^1p^*$ state) [9]. On decreasing the temperature in the high viscosity range a marked decrease in $\phi_{t\rightarrow c}$ was found for the nitrostilbenes [8-10].

5. Conclusions

Substitution of stilbene by a cyano group in the 4 position and by H, CN, CH_3O or $(CH_3)_2N$ in the 4′ position leads to remarkable effects in the absorption and emission characteristics of these compounds. However, a close similarity was found for the effect of solvent polarity on the position of the photostationary state, on $\phi_{c\rightarrow t}$ and on $\phi_{t\rightarrow c}$, for the effect of quenchers on the $^1t^*$ state, and for the effects of temperature and viscosity on ϕ_f, $\phi_{c\rightarrow t}$, $\phi_{t\rightarrow c}$, ϕ_T and τ_T. These results are interpreted in terms of a reaction scheme for the *cis*⇄*trans* photoisomerization.

It is suggested that a singlet mechanism accounts for the data and that the lowest triplet state of the cyanostilbenes is not involved in the direct *cis*⇄*trans* photoisomerization in liquid solution at room temperature. This is explained by the very small yield of intersystem crossing rather than by a short triplet lifetime. From results of sensitized *cis–trans* photoisomerization measurements it can be seen that the lowest triplet state of CMS and CDMAS [7] is populated and decays in a similar manner to that of stilbene.

The photochemical behaviour of the 4-cyanostilbenes is closely related to that of unsubstituted stilbene but is contrary to that of the corresponding 4-nitrostilbenes. For the latter compounds *trans→cis* photoisomerization occurs via the (lowest) triplet pathway. 4-Halogenated stilbenes are placed between these two classes of stilbenes. Because of the heavy atom effect the quantum yield of intersystem crossing to an upper excited triplet state is substantial for 4-bromostilbene and 4-chlorostilbene. For stilbene and 4-halogenated stilbenes the upper excited triplet pathway competes with the singlet pathway and the lowest triplet pathway [18].

Acknowledgments

The author is deeply indebted to Professor D. Schulte-Frohlinde for his continuing advice and stimulating interest and thanks Mr. H. Gruen for help-

ful discussions and Miss C. Hüsken and Mr. L. J. Currell for technical assistance. The author is also obliged to Professor Saltiel for a preprint of his review (ref. 32).

References

1 D. V. Bent and D. Schulte-Frohlinde, *J. Phys. Chem.*, *78* (1974) 446.
2 D. V. Bent and D. Schulte-Frohlinde, *J. Phys. Chem.*, *78* (1974) 451.
3 D. Schulte-Frohlinde and D. V. Bent, *Mol. Photochem.*, *6* (1974) 315.
4 M. N. Pisanias and D. Schulte-Frohlinde, *Ber. Bunsenges. Phys. Chem.*, *79* (1975) 662.
5 H. J. Kuhn, R. Straatmann and D. Schulte-Frohlinde, *J. Chem. Soc., Chem. Commun.*, (1976) 824.
6 H. Görner and D. Schulte-Frohlinde, *Ber. Bunsenges. Phys. Chem.*, *81* (1977) 713.
7 H. Görner and D. Schulte-Frohlinde, *J. Photochem.*, *8* (1978) 91.
8 H. Görner and S. Schulte-Frohlinde, *Ber. Bunsenges. Phys. Chem.*, *82* (1978) 1102.
9 H. Görner and D. Schulte-Frohlinde, *J. Phys. Chem.*, *82* (1978) 2653.
10 D. Schulte-Frohlinde and H. Görner, *Pure Appl. Chem.*, *51* (1979) 279.
11 H. Görner and D. Schulte-Frohlinde, to be published.
12 J. Saltiel and J. T. D'Agostino, *J. Am. Chem. Soc.*, *94* (1972) 6445.
13 J. Saltiel, J. T. D'Agostino, E. D. Megarity, L. Metts, K. R. Neuberger, M. Wrighton and O. C. Zafiriou, *Org. Photochem.*, *3* (1973) 1.
14 J. Saltiel, D. W.-L. Chang, E. D. Megarity, A. D. Rousseau, P. T. Shannon, B. Thomas and A. K. Uriarte, *Pure Appl. Chem.*, *41* (1975) 559.
15 A. Marinari and J. Saltiel, *Mol. Photochem.*, *7* (1976) 225.
16 J. Saltiel, A. Marinari, D. W.-L. Chang, J. C. Mitchener and E. D. Megarity, *J. Am. Chem. Soc.*, *101* (1979) 2982.
17 H. Görner and D. Schulte-Frohlinde, *J. Am. Chem. Soc.*, *101* (1979) 4388.
18 H. Görner and D. Schulte-Frohlinde, *J. Phys. Chem.*, *83* (1979) 3107.
19 G. Heinrich, S. Schoof and H. Güsten, *J. Photochem.*, *3* (1974/75) 315.
20 H. Jungmann, H. Güsten and D. Schulte-Frohlinde, *Chem. Ber.*, *101* (1968) 2690.
21 P. Pfeiffer, *Ber. Dtsch. Chem. Ges.*, *48* (1916) 1777.
G. Riezebos and E. Havinga, *Rec. Trav. Chim. Pays Bas*, *80* (1961) 446.
22 H. Görner and D. Schulte-Frohlinde, *Chem. Phys. Lett.*, *66* (1979) 363.
23 D. Schulte-Frohlinde, H. Blume and H. Güsten, *J. Phys. Chem.*, *66* (1962) 2486.
24 D. Schulte-Frohlinde, *Justus Liebigs Ann. Chem.*, *615* (1958) 114.
25 H. Güsten and L. Klasinc, *Tetrahedron Lett.*, (1968) 3097.
26 R. H. Dyck and D. S. McClure, *J. Chem. Phys.*, *36* (1962) 2326.
27 S. Malkin and E. Fischer, *J. Phys. Chem.*, *68* (1964) 1153.
28 D. Gegiou, K. A. Muszkat and E. Fischer, *J. Am. Chem. Soc.*, *90* (1968) 12.
D. Gegiou, K. A. Muszkat and E. Fischer, *J. Am. Chem. Soc.*, *90* (1968) 3907.
29 E. Lippert and F. Moll, *Z. Elektrochem.*, *58* (1954) 718.
30 E. Lippert, W. Lüder, F. Moll, W. Nägele, H. Boos, H. Prigge and I. Seibold-Blankenstein, *Angew. Chem.*, *73* (1961) 695.
31 S. Sharafy and K. A. Muszkat, *J. Am. Chem. Soc.*, *93* (1971) 4119.
32 J. Saltiel and J. L. Charlton, to be published.
33 J. Saltiel, G.-E. Khalil and K. Schanze, *Chem. Phys. Lett.*, *70* (1980) 233.
34 J. Saltiel and B. Thomas, *J. Am. Chem. Soc.*, *96* (1974) 5660.
35 B. I. Greene, R. M. Hochstrasser and R. B. Weisman, *Chem. Phys. Lett.*, *62* (1979) 427.
B. I. Greene, R. M. Hochstrasser and R. B. Weisman, *J. Chem. Phys.*, *71* (1979) 544.
K. Yoshihara, A. Namiki, M. Sumitani and N. Nakashima, *J. Chem. Phys.*, *71* (1979) 2892.
36 W. G. Herkstroeter and G. S. Hammond, *J. Am. Chem. Soc.*, *88* (1966) 4769.
37 K. A. Muszkat, H. Kessel and S. Sharafi-Ozeri, *Isr. J. Chem.*, *16* (1977) 291.